Pergamon

Int. J. Solids Structures Vol. 33, No. 9, pp. 1271–1286, 1996

0020-7683/96 $15.00 + .00

0020-7683(95)00099-2

THE FINITE DEFORMATION OF NONLINEAR COMPOSITE MATERIALS—I. INSTANTANEOUS CONSTITUTIVE RELATIONS

P. PONTE CASTAÑEDA and M. ZAIDMAN
Department of Mechanical Engineering and Applied Mechanics, University of Pennsylvania, Philadelphia, PA 19104, U.S.A.

(*Received* 21 *September* 1994; *in revised form* 14 *April* 1995)

Abstract—This work deals with the development of effective constitutive models for two-phase nonlinearly viscous and rigid–perfectly plastic composites subjected to finite deformations. The main new feature of the model is the ability to account approximately for the evolution of the microstructure resulting from the finite changes in geometry during a given deformation process. The model is formulated in terms of instantaneous constitutive relations for the composites, which depend on appropriate variables characterizing the state of the microstructure, together with evolution equations for these state variables. This first part of the work is concerned with the development of the instantaneous constitutive relations for classes of microstructures that are sufficiently broad to capture the changes in microstructure associated with general triaxial finite-deformation histories. Simple formulae are given for the effective potentials and stress–strain rate relations of power-law viscous composites made of aligned ellipsoidal inclusions of one phase dispersed in a matrix of a second phase. In addition, effective yield surfaces are computed for the special case of two-phase rigid–perfectly plastic composites with aligned spheroidal inclusions. The effects of the phase volume fractions, inclusion shape and yield strength ratio on these effective yield surfaces are considered. These effects will turn out to be important in the understanding of the effective response of the composites with evolving microstructures, which is considered in Part II of this work.

1. INTRODUCTION

During a typical forming process involving the finite deformation of an inhomogeneous metal or polymer, the geometrical arrangement of the constituent phases (i.e. the microstructure) may be significantly affected. This poses a severe limitation on the application of most homogenization models available to date (e.g. Bishop and Hill, 1951; Drucker, 1959; Hill, 1965; Hutchinson, 1976; Suquet, 1983; Bao *et al.*, 1991), which implicitly assume that the microstructure remains fixed. Following an analogous treatment for porous materials by Ponte Castañeda and Zaidman (1994), in this work we develop a constitutive model which is capable of accounting approximately for the evolution of the microstructure in two-phase nonlinearly viscous (or rigid–perfectly plastic) solids, subjected to finite deformations. Such a model takes the form of a standard homogenization model, supplemented by evolution laws for appropriate variables serving to characterize the "state" of the microstructure.

The first part of this work deals with the development of instantaneous effective potentials and stress–strain rate relations for two-phase nonlinearly viscous and rigid–perfectly plastic composites with particulate microstructures exhibiting "ellipsoidal symmetry". This class of microstructures corresponds to aligned ellipsoidal inclusions of one phase distributed in a matrix of another phase. These microstructures are useful in the present context because, as we will see in Part II of this work (Zaidman and Ponte Castañeda, 1995), they arise naturally in the analysis of the finite deformation of nonlinearly viscous composites subjected to triaxial loading conditions (with fixed axes). In addition, explicit estimates of the Hashin–Shtrikman (1963) type are available, from the work of Willis (1977, 1978), for the effective behavior of linearly viscous composites with ellipsoidal microstructures. [We note that these estimates are also associated with the names of Mori and Tanaka (1973).] These linear estimates for the effective viscosity tensor of materials with particulate ellipsoidal symmetry will be used here to generate corresponding estimates

for the effective potentials of nonlinearly viscous composites by means of the nonlinear homogenization procedure of Ponte Castañeda (1991, 1992). The resulting estimates for the effective potentials of the nonlinearly viscous composites will then be used in Part II of this work, together with appropriate evolution equations for the volume fraction and aspect ratios of the aligned ellipsoidal inclusions (which are the appropriate state variables in this case), to complete the constitutive description of the nonlinearly viscous composites under finite deformations.

2. VARIATIONAL CHARACTERIZATION OF THE EFFECTIVE BEHAVIOR OF NONLINEARLY VISCOUS COMPOSITES

For our purposes, a composite is a heterogeneous material with two distinct length scales: a macroscopic one, $L \sim O(1)$, characterizing the overall dimensions of the specimen and the scale of variation of the applied loading conditions, and a microscopic one, $l \ll L$, characterizing the size of the typical heterogeneity (e.g. an inclusion). By effective properties, we mean the relation between the averages of the local stress and strain rate fields within the composite. Below we discuss how such a relation may be obtained from the effective potential of the composite, and also how this potential function may be estimated for nonlinearly viscous composites in terms of corresponding estimates for the effective potentials of linearly viscous composites.

The local constitutive behavior of the nonlinearly viscous composites, under finite deformations, is defined by the relation

$$\mathbf{D} = \frac{\partial U}{\partial \boldsymbol{\sigma}}(\mathbf{x}, \boldsymbol{\sigma}), \tag{1}$$

where $\boldsymbol{\sigma}$ and $\mathbf{D}$ denote respectively the Cauchy stress and Eulerian strain rate (or rate-of-deformation) tensors. These are functions of position $\mathbf{x}$ in the composite, which is assumed to occupy a domain Ω (normalized to have unit volume) with boundary $\partial\Omega$. We will further assume that the composite is made up of two homogeneous phases with incompressible behavior (recall that objectivity requires that U be an isotropic function of $\boldsymbol{\sigma}$). Therefore, the strain rate potential U will be taken to be of the form

$$U(\mathbf{x}, \boldsymbol{\sigma}) = \sum_{r=1}^{2} \chi^{(r)}(\mathbf{x}) \phi^{(r)}(\sigma_e) \tag{2}$$

where the $\chi^{(r)}$ $(r = 1, 2)$ are characteristic functions of the two phases (equal to 1 if $\mathbf{x}$ is in phase r, and 0 otherwise). Note that the volume averages of the functions $\chi^{(r)}$ are the volume fractions of the phases, denoted as $c^{(r)}$. The phase potentials $\phi^{(r)}$ are taken to be convex on the equivalent stress $\sigma_e = [(3/2)\boldsymbol{\sigma}' \cdot \boldsymbol{\sigma}']^{1/2}$, where $\boldsymbol{\sigma}'$ denotes the deviatoric stress. A possible choice for the functions $\phi^{(r)}$ is the power-law form

$$\phi^{(r)}(\sigma_e) = \frac{1}{3(n^{(r)}+1)\eta^{(r)}} \sigma_e^{n^{(r)}+1} = \frac{\sigma_y^{(r)}}{(n^{(r)}+1)} \left[\frac{\sigma_e}{\sigma_y^{(r)}}\right]^{n^{(r)}+1}, \tag{3}$$

which is commonly used in high-temperature creep. In this relation, $n^{(r)}$ (in the range $[1, \infty]$) and $\sigma_y^{(r)} = (3\eta^{(r)})^{1/n^{(r)}}$ are the creep exponent and reference stress of phase r. The two limiting values of the exponent, 1 and ∞, are of special interest because they correspond, respectively, to linearly viscous behavior with viscosity $\eta^{(r)}$ and rigid–perfectly plastic behavior of the von Mises type with tensile yield stress $\sigma_y^{(r)}$. In the second case, the relation (1) is replaced by $\mathbf{D} = \dot{\lambda}(\mathbf{x})\boldsymbol{\sigma}'$, where $\dot{\lambda}$ is the plastic loading parameter.

Following Hill (1963), the effective behavior of the composite is determined by the following relation between the average (over Ω) stress $\bar{\boldsymbol{\sigma}}$ and the average strain rate $\bar{\mathbf{D}}$, namely,

$$\bar{\mathbf{D}} = \frac{\partial \tilde{U}}{\partial \bar{\boldsymbol{\sigma}}}(\bar{\boldsymbol{\sigma}}), \tag{4}$$

where $\tilde{U}$ denotes the effective strain rate potential of the composite. This effective potential may be given the variational representation:

$$\tilde{U}(\bar{\boldsymbol{\sigma}}) = \min_{\boldsymbol{\sigma} \in S(\bar{\boldsymbol{\sigma}})} \int_{\Omega} U(\mathbf{x}, \boldsymbol{\sigma})\, dv, \tag{5}$$

where

$$S(\bar{\boldsymbol{\sigma}}) = \{\boldsymbol{\sigma} | \nabla \cdot \boldsymbol{\sigma} = 0 \text{ in } \Omega, \text{ and } \boldsymbol{\sigma}\mathbf{n} = \bar{\boldsymbol{\sigma}}\mathbf{n} \text{ on } \partial\Omega\}$$

is the set of statically admissible stresses corresponding to applied uniform stress $\bar{\boldsymbol{\sigma}}$ on the boundary. In the above definition, we have implicitly assumed that the associated velocity field $\mathbf{v}$ (such that $D_{ij} = (v_{i,j} + v_{j,i})/2$) is small enough that inertial effects may be safely neglected (relative to viscous effects).

In particular, for linear behavior, the Euler–Lagrange equations (5) are precisely Stoke's equations for slow viscous flows. Then, the effective potential for the composite fluid may be written in terms of an effective viscosity tensor $\tilde{\mathbf{L}}$ (mathematically analogous to the elastic modulus tensor), or alternatively in terms of a viscous compliance tensor $\tilde{\mathbf{M}} = \tilde{\mathbf{L}}^{-1}$, such that

$$\tilde{U}(\bar{\boldsymbol{\sigma}}) = \tfrac{1}{2}\bar{\boldsymbol{\sigma}} \cdot (\tilde{\mathbf{M}}\bar{\boldsymbol{\sigma}}). \tag{6}$$

On the other hand, for rigid–perfectly plastic behavior, the governing equations may be identified with the Prandtl–Reuss equations. Then, it is convenient to introduce an effective yield domain $\tilde{P}$ (Bishop and Hill, 1951; Suquet, 1983), such that

$$\tilde{U}(\bar{\boldsymbol{\sigma}}) = \begin{cases} 0 & \text{if } \bar{\boldsymbol{\sigma}} \in \tilde{P}, \\ \infty & \text{otherwise.} \end{cases} \tag{7}$$

The boundary of $\tilde{P}$ defines an effective, or extremal, yield surface

$$\tilde{\Phi}(\bar{\boldsymbol{\sigma}}) = 0, \tag{8}$$

in terms of which (Hill, 1967) we have that

$$\bar{\mathbf{D}} = \dot{\Lambda} \frac{\partial \tilde{\Phi}}{\partial \bar{\boldsymbol{\sigma}}}(\bar{\boldsymbol{\sigma}}), \tag{9}$$

where $\dot{\Lambda}$ is a non-negative parameter that is to be determined from the consistency condition $\dot{\tilde{\Phi}} = 0$. We emphasize that $\tilde{U}$, and therefore $\tilde{\mathbf{L}}$ and $\tilde{\Phi}$, will be anisotropic for general microstructures, even though the local constitutive behavior is itself isotropic. However, it follows from the assumed convexity of U that the effective potential $\tilde{U}$ will also be convex. In particular, this implies that $\tilde{\Phi}$ will be convex.

Ponte Castañeda (1991, 1992) proposed an exact, alternative variational representation of the effective potential function (5) in terms of the effective potential functions of appropriate classes of linear comparison composites. This variational representation may be used approximately to obtain estimates for the effective potentials of classes of nonlinear composites in terms of corresponding estimates for linear composites with identical microstructures. For the class of two-phase incompressible composites defined by eqn (2), with prescribed volume fractions $c^{(1)}$ and $c^{(2)}$ (such that $c^{(1)} + c^{(2)} = 1$), the variational principle gives the following estimate for $\tilde{U}$, namely,

$$\tilde{U}(\bar{\boldsymbol{\sigma}}) \geqslant \max_{\mu^{(1)},\mu^{(2)}\geqslant 0} \left\{ \tfrac{1}{2}\bar{\boldsymbol{\sigma}} \cdot (\tilde{\mathbf{M}}\bar{\boldsymbol{\sigma}}) - \sum_{r=1}^{2} c^{(r)} V^{(r)}(\mu^{(r)}) \right\}, \tag{10}$$

where $\tilde{\mathbf{M}} = \tilde{\mathbf{M}}(\mu^{(1)}, \mu^{(2)})$ denotes any estimate for the effective viscous compliance tensor of the class of two-phase linear composites with viscosities $\mu^{(1)}$ and $\mu^{(2)}$ in prescribed volume fractions $c^{(1)}$ and $c^{(2)}$, and with the same microstructure or class of microstructures as for the given nonlinear composites. The functions $V^{(r)}$ $(r = 1, 2)$ are defined by

$$V^{(r)}(\mu^{(r)}) = \max_{\sigma} \left\{ \frac{1}{6\mu^{(r)}}\sigma_e^2 - \phi^{(r)}(\sigma_e) \right\}, \tag{11}$$

and we note, for later reference, that under the hypothesis that the functions $\phi^{(r)}$ are convex on σ_e^2 [the "strong convexity" hypothesis of Ponte Castañeda (1992)], it follows that

$$\phi^{(r)}(\sigma_e) = \max_{\mu^{(r)}} \left\{ \frac{1}{6\mu^{(r)}}\sigma_e^2 - V^{(r)}(\mu^{(r)}) \right\}. \tag{12}$$

We observe that while the inequality (10) may be useful in the context of determining bounds for the potentials $\tilde{U}$ of composites with broad classes of microstructures, it is more useful from a practical point of view to think of the right-hand-side of (10) as an estimate for the potentials of composites with specific types of microstructures, in which case the inequality (10) may be replaced by an equality (in the sense of an approximation). In particular, we are usually interested in obtaining the effective stress–strain rate relations for the composite from relations (4) or (9). Then, the inequality (10) should always be replaced by an equality, since the differentiation of an inequality does not preserve, in general, the sense of the inequality.

The optimal values of $\mu^{(1)}$ and $\mu^{(2)}$ in the estimate (10) are denoted by $\hat{\mu}^{(1)}$ and $\hat{\mu}^{(2)}$, respectively, and are normally determined by the optimality conditions

$$\tfrac{1}{2}\bar{\boldsymbol{\sigma}} \cdot \left[\frac{\partial \tilde{\mathbf{M}}}{\partial \mu^{(s)}}(\hat{\mu}^{(1)}, \hat{\mu}^{(2)})\bar{\boldsymbol{\sigma}} \right] - c^{(s)} \frac{\partial V^{(s)}}{\partial \mu^{(s)}}(\hat{\mu}^{(s)}) = 0, \quad (s = 1, 2). \tag{13}$$

In this case, it was shown by deBotton and Ponte Castañeda (1993) that the effective stress–strain rate relation (4) reduces to

$$\bar{\mathbf{D}} = \tilde{\mathbf{M}}(\hat{\mu}^{(1)}, \hat{\mu}^{(2)})\bar{\boldsymbol{\sigma}}. \tag{14}$$

We emphasize that, in spite of its appearance, the constitutive relation (14) is fully nonlinear—because of the dependence of $\hat{\mu}^{(1)}$ and $\hat{\mu}^{(2)}$ on $\bar{\boldsymbol{\sigma}}$. However, relation (14) shows that it may be useful to think of the nonlinearly viscous composite as a linearly viscous composite with stress-dependent viscosities $\hat{\mu}^{(1)} = \hat{\mu}^{(1)}(\bar{\boldsymbol{\sigma}})$ and $\hat{\mu}^{(2)} = \hat{\mu}^{(2)}(\bar{\boldsymbol{\sigma}})$, as determined by the optimality conditions (13).

In the following sections, we will make use of appropriate estimates for the effective behavior of the class of two-phase linearly viscous composites with particulate microstructures (i.e. with clearly defined matrix and inclusion phases) to generate corresponding estimates for the effective behavior of nonlinearly viscous and rigid–perfectly plastic composites. It is important to emphasize at this stage that these estimates for the potentials (yield surfaces) of the nonlinearly viscous (rigid–perfectly plastic) composites hold at fixed microstructures. Naturally, when the composite undergoes a finite deformation program, the microstructure evolves. For this reason, in the next section we will develop estimates for families of microstructures that are broad enough to capture the sequence of microstructures that a composite would undergo, as the deformation progresses, under general triaxial loading conditions (without rotation of the axes). These estimates will be used in

Part II of this work, together with evolution equations for appropriate state variables characterizing the state of the microstructure.

3. THE EFFECTIVE BEHAVIOR OF COMPOSITES WITH PARTICULATE MICROSTRUCTURES

The assumption of statistical homogeneity and isotropy led Hashin and Shtrikman (1963) to the development of explicit estimates, in the form of rigorous upper and lower bounds, for the effective behavior of composites with random distributions of linear elastic (or, taking advantage of a well-known analogy, linearly viscous) phases. These variational estimates have been identified with different types of optimal microstructures [see, for example, Milton and Kohn (1988)], which have the topological property of containing dispersions of inclusions of one phase in a continuous matrix of the other (i.e. particulate microstructures). In these optimal microstructures, it is found that the upper (lower) bound for the effective stiffness tensor corresponds to choosing the stiffer phase to play the role of the matrix (inclusion), and the more compliant phase the role of the inclusion (matrix). In another seminal contribution, Willis (1977) introduced the notion of "ellipsoidal symmetry" and obtained a generalization of the Hashin–Shtrikman bounds for the class of microstructures with this more general type of statistical symmetry. Microstructures with ellipsoidal symmetry are essentially stretched versions of statistically isotropic microstructures. Special cases of these microstructures are those made up of aligned, self-similar ellipsoidal inclusions [with aspect ratios $w_1 = l_3/l_1$ and $w_2 = l_3/l_2$; see Fig. 1(a)] of one phase dispersed in a matrix of another, in such a way that the two-point correlation functions characterizing the distribution of the centers of the inclusions are also ellipsoidal [with "aspect ratios" L_3/L_1 and L_3/L_2 equal to w_1 and w_2, respectively; see Fig. 1(b)]. Note that microstructures with general ellipsoidal symmetry may include the case where the phases are distributed in such a way that there are no clearly defined matrix and inclusion phases. However, it has been shown [see Willis (1978)] that the expressions for the bounds of Willis (1977), for general classes of microstructures with ellipsoidal symmetry, serve as actual variational estimates for the subclass of particulate microstructures with ellipsoidal symmetry (with aligned ellipsoidal inclusions), in such a way that the upper (lower) bound corresponds once again to the microstructures, with the stiffer and more compliant materials occupying the matrix (inclusion) and inclusion (matrix) phases, respectively.

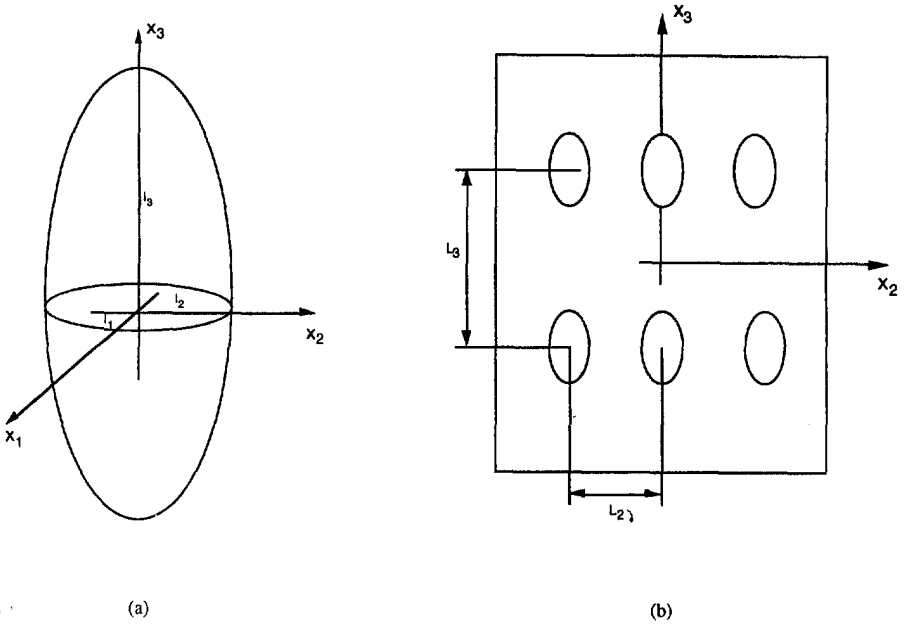

(a) (b)

Fig. 1. Schematic representation of the inclusion geometry and distribution. The distribution is depicted as being rectangular for illustrative purposes only.

Because of the above arguments, in this work we will make use of the estimates of Willis (1977, 1978) for linear composites with particulate microstructures to generate, via the variational statement (10), corresponding estimates for the effective behavior of nonlinearly viscous composites with particulate microstructures. In the first subsection here, we briefly recall the estimates of Willis (1977, 1978), and in the following one, we apply these estimates to the special case of nonlinearly viscous composites with phase behaviors as given by eqn (3) with $n^{(1)} = n^{(2)} = n$ (pure power-law behavior).

3.1. *Linear composites with particulate microstructures*

For the class of two-phase composites with prescribed volume fractions $c^{(1)}$ and $c^{(2)}$, phase viscosity tensors $\mathbf{L}^{(1)}$ and $\mathbf{L}^{(2)}$, and particulate microstructures as defined above, the estimate of Willis (1977, 1978) may be expressed in the form

$$\tilde{\mathbf{M}} = \{\mathbf{I} + c^{(1)}[(\mathbf{M}^{(1)}\mathbf{L}^{(2)} - \mathbf{I})^{-1} + c^{(2)}(\mathbf{I} - \mathbf{S}^{(2)})]^{-1}\}\mathbf{M}^{(2)}, \tag{15}$$

where we have chosen material 2 to occupy the matrix phase. In this expression, $\mathbf{S}^{(2)}$ denotes the Eshelby (1957) tensor associated with an isolated ellipsoidal inclusion with aspect ratios $w_1 = l_3/l_1$ and $w_2 = l_3/l_2$ [see Fig. 1(a)], embedded in a matrix of phase 2. As already mentioned, this estimate may also be interpreted as an upper (lower) bound for $\tilde{\mathbf{M}}$ (in the sense of quadratic forms) for the general class of composites with ellipsoidal symmetry if $\mathbf{M}^{(1)} < \mathbf{M}^{(2)}$ ($\mathbf{M}^{(1)} > \mathbf{M}^{(2)}$).

It is well known that the above estimate for $\tilde{\mathbf{M}}$ is exact for dilute concentrations of inclusions ($c^{(1)} \ll 1$); we can verify that it reduces to the dilute estimate of Eshelby (1957) by simply replacing the factor $c^{(2)}$ by 1 in the above expression. Thus, the estimate (15) serves as a generalization of Eshelby's estimates for particulate composites with dilute concentrations of inclusions to particulate composites with nondilute concentrations of inclusions. We emphasize that the above estimates are only appropriate for particulate microstructures with "ellipsoidal symmetry". They would not be appropriate, for example, for periodic microstructures, which exhibit a "packing" limit for volume fraction of inclusions less than 100%.

3.2. *Pure power-law viscous composites with particulate microstructures*

In this section, we make use of the result (15) for linearly viscous composites, specialized to isotropic, incompressible constituents, to generate via (10) estimates for the effective potential of nonlinearly viscous composites with pure power-law constituents of the type described by eqn (3) with $n^{(1)} = n^{(2)} = n$. In order to simplify the expression (10) for this case, we make the following two observations. First, by virtue of the incompressibility and isotropy of the phases of the linear comparison composite, $\tilde{\mathbf{M}}$, as given by eqn (15), may be written in the form

$$\tilde{\mathbf{M}} = \frac{1}{3\mu^{(2)}}\tilde{\mathbf{m}}(y^{(1)}), \tag{16}$$

where $\tilde{\mathbf{m}}$ depends on the linear comparison viscosities $\mu^{(1)}$ and $\mu^{(2)}$ only through the ratio $y^{(1)} = (y^{(2)})^{-1} = \mu^{(2)}/\mu^{(1)}$. Second, because of the pure power-law hypothesis, we have, from eqn (11), that

$$V^{(1)}(\mu^{(1)}) = \frac{(n-1)}{2(n+1)}\frac{(\sigma_y^{(1)})^{2n/(n-1)}}{(3\mu^{(1)})^{(n+1)/(n-1)}} = (z^{(2)})^{2n/(n-1)}(y^{(1)})^{(n+1)/(n-1)}V^{(2)}(\mu^{(2)}), \tag{17}$$

where $z^{(2)} = (z^{(1)})^{-1} = \sigma_y^{(1)}/\sigma_y^{(2)}$ is the ratio of the reference stresses of the two phases.

It then follows that expression (10) may be rewritten in the form

$$\tilde{U}(\bar{\boldsymbol{\sigma}}) \geqslant \max_{y^{(1)} \geqslant 0} \left\{ [c^{(2)} + c^{(1)}(z^{(2)})^{2n/(n-1)}(y^{(1)})^{(n+1)/(n-1)}] \max_{\mu^{(2)} \geqslant 0} \left\{ \frac{1}{6\mu^{(2)}}(\hat{\sigma}_e^{(1)})^2 - V^{(2)}(\mu^{(2)}) \right\} \right\}, \tag{18}$$

where

$$\hat{\sigma}_e^{(1)}(y^{(1)}) = \sqrt{[c^{(2)} + c^{(1)}(z^{(2)})^{2n/(n-1)}(y^{(1)})^{(n+1)/(n-1)}]^{-1}\bar{\boldsymbol{\sigma}} \cdot [\tilde{\mathbf{m}}(y^{(1)})\bar{\boldsymbol{\sigma}}]}, \tag{19}$$

from which it follows, via eqn (12), that

$$\tilde{U}(\bar{\boldsymbol{\sigma}}) \geqslant \max_{y^{(1)} \geqslant 0} \{ [c^{(2)} + c^{(1)}(z^{(2)})^{2n/(n-1)}(y^{(1)})^{(n+1)/(n-1)}] \phi^{(2)}[\hat{\sigma}_e^{(1)}(y^{(1)})] \}. \tag{20}$$

These results for power-law composites may be specialized for rigid–perfectly plastic composites, by noting that

$$\phi^{(2)}(\sigma_e) = \begin{cases} 0 & \text{if } \sigma_e \leqslant \sigma_y^{(2)}, \\ \infty & \text{otherwise,} \end{cases} \tag{21}$$

which leads to the conclusion that

$$\tilde{\Phi}(\bar{\boldsymbol{\sigma}}) \leqslant \max_{y^{(1)} \geqslant 0} \{ [c^{(2)} + c^{(1)}(z^{(2)})^2 y^{(1)}]^{-1} \bar{\boldsymbol{\sigma}} \cdot [\tilde{\mathbf{m}}(y^{(1)})\bar{\boldsymbol{\sigma}}] - (\sigma_y^{(2)})^2 \} \equiv \tilde{\Phi}^{(+)}(\bar{\boldsymbol{\sigma}}). \tag{22}$$

We note that relations (20) and (22) respectively provide the desired generalization to power-law viscous and rigid–perfectly plastic composites of expression (15) for the linearly viscous composites with particulate microstructures. Unlike eqn (15), these expressions are not explicit, but involve one-dimensional optimization problems for the ratio $y^{(1)} = \mu^{(2)}/\mu^{(1)}$, which are simpler than the general form (10) involving a two-dimensional optimization.

Next, we observe that, as was the case for eqn (15), the estimate (20) may be interpreted as a rigorous lower bound for $\tilde{U}$ for the class of power-law composites with general ellipsoidal symmetry if $\sigma_y^{(1)} < \sigma_y^{(2)}$. However, due to the direction of the inequality (10), (20) fails to provide a rigorous upper bound for $\tilde{U}$ if $\sigma_y^{(1)} > \sigma_y^{(2)}$ (for the class of composites with general ellipsoidal symmetry). Similarly, the yield surfaces obtained from estimates (22) by setting $\tilde{\Phi}^{(+)}(\bar{\boldsymbol{\sigma}}) = 0$ provide rigorous upper bounds for the yield surfaces of composites with ellipsoidal microstructures if $\sigma_y^{(1)} < \sigma_y^{(2)}$, but they do not provide rigorous lower bounds for the yield surfaces if, on the other hand, $\sigma_y^{(1)} > \sigma_y^{(2)}$.

Nevertheless, comparisons with experiments and numerical simulations for metal–matrix composites [see, for example, Figs 3, 4 and 5 of Li and Ponte Castañeda (1994) and also Fig. 3 of the present work] have shown that expressions of the type (20) and (22) (with the inequalities replaced by equalities, as explained in Section 2) provide reasonably accurate estimates for the effective behavior of nonlinear composite materials with particulate microstructures. In addition, the agreement is not only good for the effective potentials, but also, more importantly, for the associated stress–strain rate relations. Because of these observations, we will make use of expressions (20) and (22) (with the inequalities replaced by equalities) and of relations (4) and (9) [or relation (14)] as estimates (not bounds) for the effective potentials and stress–strain rate relations, respectively, of composites with particulate microstructures, with material 1 occupying the inclusion phase and material 2 the matrix phase.

Estimates of the type (20) for two-phase power-law viscous composites, with overall isotropic symmetry, were obtained by Ponte Castañeda (1991, 1992). The corresponding estimates for two-phase rigid–perfectly plastic composites with isotropic and transversely

isotropic (laminated and fiber-reinforced) microstructures were obtained by Ponte Castãneda and deBotton (1992). The last reference made use of the dual formulation of (10) in terms of the energy dissipation function to obtain different, but equivalent, one-dimensional representations for the effective potentials and yield functions of the nonlinear composites. The above results thus generalize the earlier ones to the more general case of particulate microstructures with aligned, ellipsoidal inclusions.

Earlier results for the special cases of porous and rigidly reinforced composites were obtained by Ponte Castañeda and Willis (1988), for composites with statistically isotropic microstructures, using the Talbot and Willis (1985) nonlinear extension of the Hashin–Shtrikman variational principles. Talbot and Willis (1992) generated the corresponding results for composites with ellipsoidal symmetry using a generalization of the Ponte Castañeda (1991) procedure. In addition, Suquet (1993) and Olson (1994) have introduced alternative variational representations for the effective behavior of power-law and rigid–perfectly plastic composites, from which they have been able to derive some the above-mentioned estimates, as well as to obtain new results.

The variational representation of Suquet exploits directly the homogeneity property of power-law materials, but unlike the representation (10), it only applies to this special class of materials. In the development of the estimates (20) and (22), from the general estimates (10), we have also exploited the homogeneity property of the power-law composite, as made explicit by relation (17). It can be shown that the specific estimates (20) and (22) also follow, perhaps more directly, from the procedure of Suquet (1993). We chose to start from the more general representation (10) because this representation may be used to generate results, albeit less simple, for the case where, for example, the two phases have different exponents. Finally, it is perhaps relevant to mention here that a generalization of the argument used in the development that led to relations (20) and (22) may be used to show that the variational principle of Suquet (1993) is strictly a special case, for pure power-law materials, of the variational principle of Ponte Castañeda (1991, 1992).

4. APPLICATION TO COMPOSITES WITH ALIGNED SPHEROIDAL INCLUSIONS

An important special case of the microstructures described in the previous section is that corresponding to spheroidal shapes for the inclusions. In this case, the aspect ratios of the inclusions become identical, such that $w_1 = w_2 = w$ [see Fig. 1(a)]. Important cases of this class of particulate microstructures are statistically isotropic ($w = 1$), laminated ($w = 0$) and fiber-reinforced ($w = \infty$) composites. In Part II of this work, we will consider the response of initially isotropic composites subjected to axisymmetric loading conditions, and we will make hypotheses that are equivalent to the assumption that the shape of the inclusions in the composite evolves in time in such a way that w varies continuously from one to zero in compression, or to infinity in tension, according to appropriate evolution laws for w. This provides one important reason for considering this class of microstructures explicitly in this section. Of course, this class of microstructures is important of its own accord, because they occur commonly in metal–matrix composites.

We note that this class of composites with spheroidal inclusions exhibits overall transversely isotropic symmetry, so that the effective potential (20) and yield function (22) may be expressed in terms of the quadratic, incompressible, transversely isotropic invariants of the stress; they are (see Fig. 1): the axisymmetric deviatoric stress $\bar{\tau}_d = 1/\sqrt{3}[\bar{\sigma}_{33} - \frac{1}{2}(\bar{\sigma}_{11} + \bar{\sigma}_{22})]$, the transverse shear stress $\bar{\tau}_p = \sqrt{\bar{\sigma}_{12}^2 + \frac{1}{4}(\bar{\sigma}_{11} - \bar{\sigma}_{22})^2}$ and the longitudinal shear stress $\bar{\tau}_n = \sqrt{\bar{\sigma}_{13}^2 + \bar{\sigma}_{23}^2}$. In terms of these invariants, we may write, from eqn (15), that

$$\tfrac{1}{2}\bar{\boldsymbol{\sigma}} \cdot (\tilde{\mathbf{M}}\bar{\boldsymbol{\sigma}}) = \frac{1}{2\tilde{\mu}_p}\bar{\tau}_p^2 + \frac{1}{2\tilde{\mu}_n}\bar{\tau}_n^2 + \frac{1}{2\tilde{\mu}_d}\bar{\tau}_d^2, \tag{23}$$

where the expressions for $\tilde{\mu}_p$, $\tilde{\mu}_n$ and $\tilde{\mu}_d$ are given explicitly in the Appendix. Making use of these expressions, together with eqn (16), we are able to rewrite the previous expression in the form

$$\tfrac{1}{3}\bar{\boldsymbol{\sigma}}\cdot[\tilde{\mathbf{m}}(y^{(1)})\bar{\boldsymbol{\sigma}}] = \frac{e_1^{(2)}y^{(1)}+e_2^{(2)}}{e_3^{(2)}y^{(1)}+e_4^{(2)}}\bar{\tau}_p^2 + \frac{f_1^{(2)}y^{(1)}+f_2^{(2)}}{f_3^{(2)}y^{(1)}+f_4^{(2)}}\bar{\tau}_n^2 + \frac{g_1^{(2)}y^{(1)}+g_2^{(2)}}{g_3^{(2)}y^{(1)}+g_4^{(2)}}\bar{\tau}_d^2, \tag{24}$$

where the expressions for the variables $e_i^{(2)}, f_i^{(2)}$ and $g_i^{(2)}$ $(i = 1, 2, 3, 4)$ are given, as functions of $y^{(1)}$, $c^{(1)}$, $c^{(2)}$ and w, by eqns (A2)–(A4) of the Appendix.

The effective yield surfaces of the rigid–perfectly plastic composites with aligned spheroidal inclusions are thus obtained by making use of eqn (24) in expression (22) for $\tilde{\Phi}$. [An exactly analogous procedure, making use of (20) instead of (22), would give results for power-law viscous composites, but this is not pursued here.] It is noted that these surfaces will be three-dimensional (with axes in stress space $\bar{\tau}_p$, $\bar{\tau}_n$ and $\bar{\tau}_d$). Below, we give results for two-dimensional cross-sections of these yield surfaces for given values of $z^{(2)} = \sigma_y^{(1)}/\sigma_y^{(2)}$, $c^{(1)}$, $c^{(2)}$ and w. In addition, we explore the dependence of the single-mode yield strengths for the composites as functions of $z^{(2)}$, $c^{(1)}$ and w.

By single-mode yield strength, we mean the effective strength of the composite when the stress components for the other two modes are set equal to zero. For example, the transverse shear yield strength is the value of the component of the stress $\bar{\tau}_p$ at which the composite yields when $\bar{\tau}_n = \bar{\tau}_d = 0$. For a composite with phase 2 in the matrix and phase 1 in the inclusion, we obtain, from relation (22) with (24), the result that

$$\left(\frac{\tilde{\tau}_p}{\tau_y^{(2)}}\right)^2 = \min_{y^{(1)}\geqslant 0}\left\{[c^{(2)}+c^{(1)}(z^{(2)})^2y^{(1)}]\left[\frac{e_3^{(2)}y^{(1)}+e_4^{(2)}}{e_1^{(2)}y^{(1)}+e_2^{(2)}}\right]\right\}. \tag{25}$$

The explicit expression for the optimal value of $y^{(1)}$ in eqn (25), denoted $\hat{y}_p^{(1)}$, is given by (ignoring the negative root):

$$\hat{y}_p^{(1)} = \frac{c^{(2)}(e_1^{(2)}e_4^{(2)}-e_2^{(2)}e_3^{(2)})-c^{(1)}e_2^{(2)}e_4^{(2)}(z^{(2)})^2}{c^{(1)}e_2^{(2)}e_3^{(2)}(z^{(2)})^2+z^{(2)}[c^{(1)}e_3^{(2)}(e_2^{(2)}e_3^{(2)}-e_1^{(2)}e_4^{(2)})(c^{(1)}e_2^{(2)}(z^{(2)})^2-c^{(2)}e_1^{(2)})]^{1/2}}, \tag{26}$$

or by $\hat{y}_p^{(1)} = 0$, depending on whether $z^{(2)}$ is smaller or greater than a certain critical value, denoted $z_p^{(2)}$. This critical value of $z^{(2)}$ is obtained by setting $\hat{y}_p^{(1)} = 0$ in eqn (26) (recall that $\hat{y}_p^{(1)}$ is constrained to be greater than zero) to obtain

$$z_p^{(2)} = \sqrt{\frac{c^{(2)}(e_1^{(2)}e_4^{(2)}-e_2^{(2)}e_3^{(2)})}{c^{(1)}e_2^{(2)}e_4^{(2)}}}. \tag{27}$$

It is also easy to see that, for $z^{(2)} \geqslant z_p^{(2)}$,

$$\tilde{\tau}_p = \sqrt{\frac{c^{(2)}e_4^{(2)}}{e_2^{(2)}}}\tau_y^{(2)}. \tag{28}$$

This last result has an interesting physical interpretation. It states that if the inclusions (phase 1) are sufficiently strong, relative to the matrix (phase 2), i.e. if $z^{(2)} \geqslant z_p^{(2)}$, then the effective yield strength of the composite will be independent of the yield strength of the stronger (inclusion) phase. In other words, according to this model, increasing the yield strength of the inclusion phase in a rigid–perfectly plastic composite will have a limited (but finite) effect on the effective yield strength of the composite. After a certain level of strengthening, the inclusions will look effectively rigid (i.e. $\hat{y}_p^{(1)} = 0$) to the composite.

The corresponding results for $\tilde{\tau}_n$ and $\tilde{\tau}_d$, as well as those for $\hat{y}_n^{(1)}, \hat{y}_d^{(1)}, z_n^{(2)}$ and $z_d^{(2)}$, have identical forms, with the functions $e_i^{(2)}$ replaced by the functions $f_i^{(2)}$ and $g_i^{(2)}$, respectively. The results for the special cases of laminates ($w = 0$), spheres ($w = 1$) and fibers ($w = \infty$) are collected for the convenience of the reader in the Appendix.

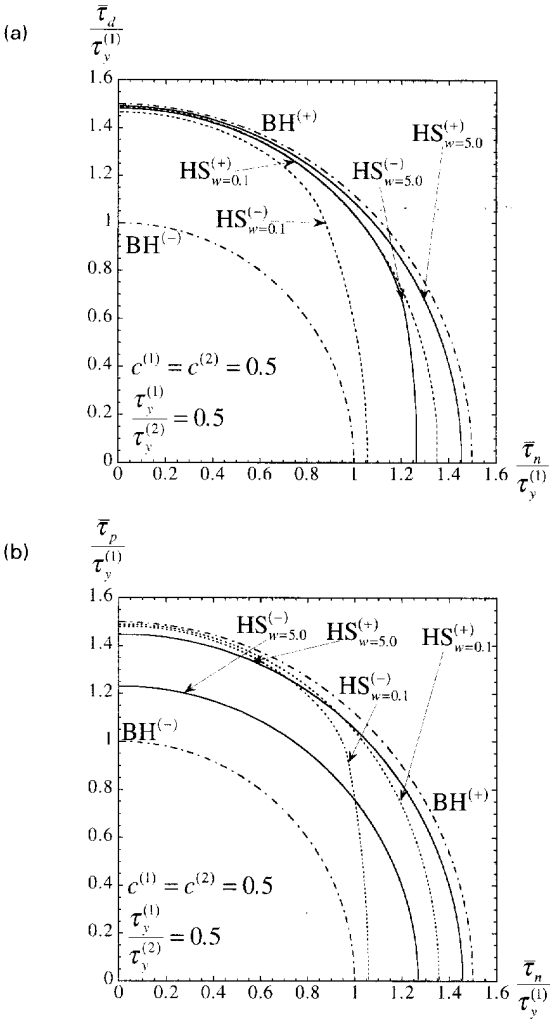

Fig. 2. Plots of two different cross-sections for the yield surfaces of two-phase composites with rigid–perfectly plastic phases and aligned spheroidal inclusions with variable aspect ratio w. The curves labeled BH(+) and BH(−) correspond to the Bishop–Hill upper and lower bounds. The curves HS(+) and HS(−) correspond to the new nonlinear Hashin–Shtrikman estimates with the stronger (2) and weaker materials (1), respectively, occupying the matrix phase. (a) $\bar{\tau}_p = 0$; (b) $\bar{\tau}_d = 0$.

The results for different two-dimensional cross-sections of these surfaces are plotted in Fig. 2 for two different values of w (0.1 and 5). The results in these figures are normalized relative to the yield strength in shear of phase 1, namely, $\tau_y^{(1)} = \sigma_y^{(1)}/\sqrt{3}$. The ratio of the yield strengths of the phases $r^{(2)} = \sigma_y^{(1)}/\sigma_y^{(2)}$ is taken to be 0.5, and the proportions of the two phases equal ($c^{(1)} = c^{(2)} = 0.5$). Given that $\sigma_y^{(1)} < \sigma_y^{(2)}$, the result of using (22) is an upper bound for the yield surfaces, denoted HS(+), which corresponds to the choice of the stronger material for the matrix phase in the composites with particulate microstructures. The results for the lower estimate, denoted HS(−), and corresponding to the choice of the weaker material for the matrix phase in the composites with particulate microstructures are obtained by interchanging the roles of the superscripts (1) and (2) in expression (22). In addition, in these plots, we provide, for comparison, the isotropic upper and lower bounds of Bishop and Hill (1951); they are denoted by BH(+) and BH(−), and are equal to the arithmetic average and minimum of the yield strengths of the two phases, respectively.

Figures 2(a) and (b) give, as examples, the $\bar{\tau}_p = 0$ and $\bar{\tau}_d = 0$ cross-sections of the yield surfaces. It is observed that all the new estimates (HS+ and −) lie within the classical bounds (BH+ and −), as they should. However, unlike the classical bounds, which are

isotropic (they appear as segments of a circle in the figures), the HS estimates are anisotropic, in general. Thus, although the HS estimates are nearly isotropic for certain types of loadings, such as combined $\bar{\tau}_p - \bar{\tau}_n$ loading for the composite with long prolate ($w = 5$) inclusions, or combined $\bar{\tau}_d - \bar{\tau}_p$ loading for the composite with flat oblate ($w = 0.1$) inclusions (not shown), the HS estimates, especially the HS($-$) estimates, may also be strongly anisotropic for other types of loadings, such as combined $\bar{\tau}_d - \bar{\tau}_n$ and $\bar{\tau}_p - \bar{\tau}_n$ loadings for the composite with $w = 0.1$, or combined $\bar{\tau}_d - \bar{\tau}_n$ and $\bar{\tau}_d - \bar{\tau}_p$ (not shown) loadings for the composite with $w = 5$.

These results may be best understood by comparing them with the results of Ponte Castañeda and deBotton (1992) for the limiting cases of laminated and fiber-reinforced composites, where it is argued that these composites, with continuous reinforcements, have weak and strong modes of deformation [see also Hashin (1980)]. The weak mode for the laminates is shear parallel to the layers ($\bar{\tau}_n \neq 0$); the corresponding weak modes for the fiber-reinforced composites are shear transverse and along the fibers ($\bar{\tau}_p \neq 0$, $\bar{\tau}_n \neq 0$), but only for the case where the matrix phase is weaker than the fiber phase. In fact, these authors found that the yield surfaces exhibit "flat sectors" at or near these weak modes, in agreement with experimental evidence [see, for example, Dvorak *et al.* (1988)]. Thus, comparison of Fig. 2 (here) and Figs 3 and 4 of Ponte Castañeda and deBotton (1992) (see also Fig. 3 of this work) shows that the yield surfaces of the flat, oblate inclusions are consistent with those of the laminate composite, and correspondingly, the yield surfaces of the composite with long, prolate inclusions are consistent with those of the fiber-reinforced composite. However, unlike the yield surfaces of the laminated and fiber composites, the yield surfaces of the particulate composite do not exhibit flat sectors (although the appropriate sectors of the yield surfaces appear to be approaching flat sectors). In fact, our experience indicates that the yield surfaces can have flat sectors only for the cases of continuous reinforcement (essentially fiber-reinforced composites with elliptical cross-sections, which range from laminated to fiber-reinforced composites).

In Fig. 3, we present plots of the $\bar{\tau}_n = 0$ cross-section of the yield surfaces for a fiber-reinforced composite with equal proportions of the phases, but with varying yield stress ratios, such that $0.1 \leqslant z^{(1)} \leqslant 2$. (The result is the same if $\bar{\tau}_p$ is replaced by $\sqrt{\bar{\tau}_p^2 + \bar{\tau}_n^2}$.) These plots are shown as continuous lines, and in them, material 2 is chosen to occupy the matrix phase, with the results being normalized relative to the yield strength of the matrix phase. It is observed that when the yield strength of the matrix is stronger than, or close to, that of the fiber ($z^{(1)} > z_p^{(1)}$; or, equivalently, $z^{(2)} < z_p^{(2)}$), the yield surfaces predicted by the model are "elliptic" in shape. However, when the matrix is sufficiently weaker than the inclusion phase ($z^{(1)} \leqslant z_p^{(1)} = \frac{1}{2}\sqrt{1+c^{(1)}}$), the yield surfaces are "bi-modal" [see Dvorak and Bahei-El-Din (1987)] in shape, with a flat sector perpendicular to the $\bar{\tau}_p$ axis ($\bar{\tau}_p = \sqrt{1+c^{(1)}\tau_y^{(2)}}$) and a curved sector roughly perpendicular to it. The relative importance of the flat sector becomes more pronounced for larger contrast, while the curved sector becomes more flat, in such a way that the yield surface becomes nearly rectangular for large enough contrast ($z^{(1)} = 0.1$, which is a reasonable number for a metal–matrix composite). Regarding the resemblance of our yield surfaces with the bi-modal yield surfaces of Dvorak

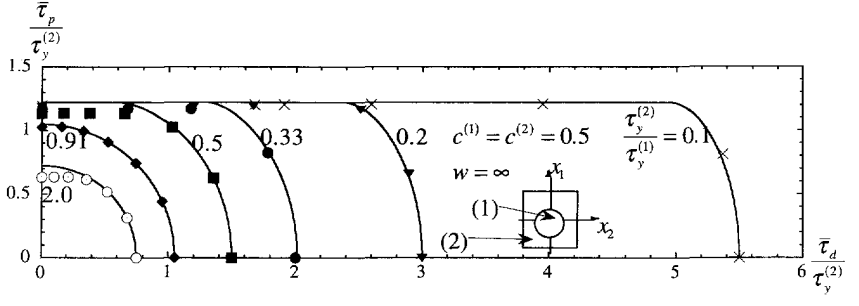

Fig. 3. Comparison of the HS estimates for the effective yield surfaces of two-phase fiber-reinforced composites ($w = \infty$) with the numerical simulations of Moulinec and Suquet (1994b) for various yield strength ratios.

and Bahei-El-Din (1987), it is worth emphasizing that the bi-modal shape for our yield surfaces is a consequence of the model and is not assumed *a priori* as in the model of Dvorak and Bahei-El-Din (1987). In addition, the present model requires only the yield strengths and volume fractions of the two phases (no measurements of the actual fiber composite are required).

Also shown in Fig. 3, in the form of different shape dots, corresponding to the different contrasts considered above, are the results of the numerical simulations of Moulinec and Suquet (1994a, b) for a quasi-random fiber composite (a periodic model with a relatively large number, about 16, of fibers thrown at random on the unit cell). It is observed that the predictions of our model are in good agreement with the numerical simulations of Moulinec and Suquet, at least for the specific configuration selected. In particular, the numerical simulations also predict a bi-modal shape, with a flat sector, for the yield surface, if the contrast of the phases is sufficiently large. However, although the numerical simulations predict that the intercept of the flat sectors with the $\tilde{\tau}_p$ axis depends (weakly) on the contrast, it has been shown that our corresponding predictions for the intercepts are insensitive to the contrast, provided that $z^{(1)}$ is sufficiently small. Two additional comments, regarding the numerical simulations, are that they are numerically intensive (a fraction of an hour on a CRAY YMP for one yield surface), whereas our predictions are explicit up to a one-dimensional optimization problem (requiring negligible computations), and that the numerical simulations are sensitive to different configurations of the fibers on the cell, yielding differences of up to 10%. These differences may be associated with different flow fields on the cell corresponding to how effective the distribution of the fibers is in blocking the development of shear bands [see Moulinec and Suquet (1994b)]. Our results are found to be in better agreement with the configurations that are more effective in blocking the development of the shear bands.

Figure 4 presents results for the dependence of the single-mode yield strengths, normalized relative to the yield strength of the stronger phase, as functions of the aspect ratio (w), the volume fraction ($c^{(1)}$) and the yield strength ratio ($z^{(2)} = \sigma_y^{(1)}/\sigma_y^{(2)}$). Figure 4(a) shows the dependence of the single-mode yield strengths on w for $c^{(1)} = c^{(2)} = 0.5$ and $z^{(2)} = 0.25$. We use the superscripts $(+)$ and $(-)$ to indicate whether they correspond to putting the stronger material (phase 2) in the matrix or in the inclusion phase. The following observations are in order. First, the dependence on w is rather strong for $\tilde{\tau}_p^{(-)}$, $\tilde{\tau}_d^{(-)}$ and $\tilde{\tau}_n^{(+)}$; on the other hand, it is relatively weak for the other three cases, with $\tilde{\tau}_p^{(+)}$, $\tilde{\tau}_d^{(+)}$ being near the arithmetic average of the yield strengths of the two phases and $\tilde{\tau}_n^{(-)}$ being near the minimum of the two yield strengths. Second, the optimal values of the strength occur at fairly different values of w for the different modes, with $w = 0$ sometimes giving the optimum, and on other occasions $w = \infty$ giving the optimum. On the other hand, the optimum may occur for an intermediate value of w, close to, but not identically equal to, 1. Space considerations prevent us from describing these findings in more detail, but the most important conclusion is that the optimal shape of the particle depends strongly on the specific loading conditions applied to the composite.

Figure 4(b) gives the dependence of the single-mode yield strengths on $z^{(2)}$ for $c^{(1)} = c^{(2)} = 0.5$ and $w = 5$. The results for the upper $(+)$ estimates show the expected behavior with decreasing strength for increasing contrast (decreasing $z^{(2)}$). However, the lower $(-)$ estimates exhibit a bilinear type of behavior, analogous to that observed by Ponte Castañeda and deBotton (1992) for the corresponding statistically isotropic composites ($w = 1$). For small enough contrast ($z^{(2)}$ sufficiently close to 1), the predictions of the lower estimates are close to those of the upper estimates just described. However, for values of $z^{(2)}$ smaller than the critical value $z_c^{(2)}$ (where the subscript c = p, n, d depends on the mode), the effective yield strength becomes independent of the yield strength of the stronger (inclusion) phase, as already observed above. This interesting phenomenon is manifested by the straight line segments in the plots for values of $z^{(2)}$ between 0 and $z_c^{(2)}$. (Note that $z_c^{(2)}$ depends on w and $c^{(1)}$.)

Figure 4(c) gives plots of the critical values of $z^{(1)} = (z^{(2)})^{-1}$, for the three different modes ($z_p^{(1)}, z_n^{(1)}, z_d^{(1)}$), as functions of w for $c^{(1)} = 0.2$ ($c^{(2)} = 0.8$). The analytical expression for $z_p^{(2)}$ is given by eqn (27) for the case where the inclusion and matrix phases are assumed

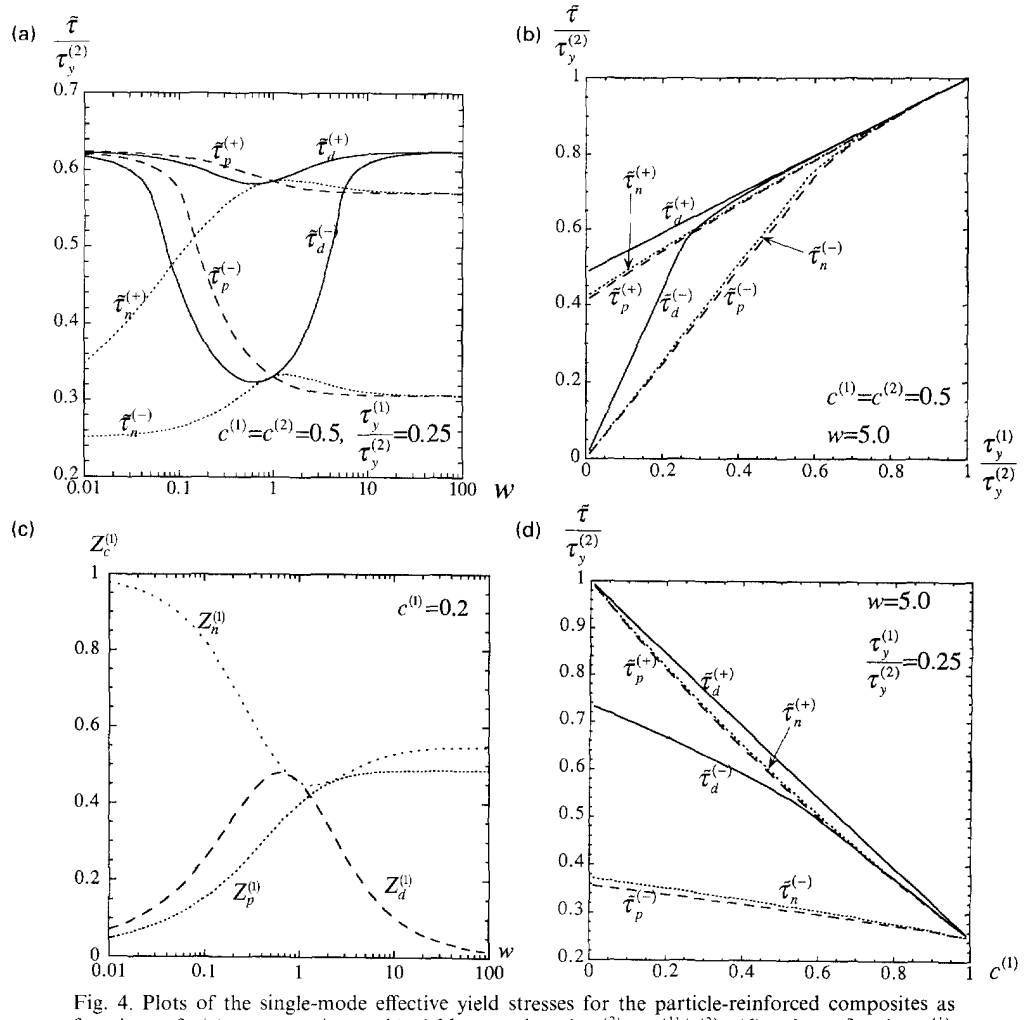

Fig. 4. Plots of the single-mode effective yield stresses for the particle-reinforced composites as functions of: (a) aspect ratio w; (b) yield strength ratio $z^{(2)} = \sigma_y^{(1)}/\sigma_y^{(2)}$; (d) volume fraction $c^{(1)}$. The "upper" estimates, denoted by (+), correspond to composites with the stronger phase (2) in the matrix and the "lower" estimates, denoted by (−), to composites with the weaker phase (1) in the matrix. The dependence of the critical value of $z^{(1)} = (z^{(2)})^{-1}$, for the three different modes, as functions of w is given in (c).

to be denoted 1 and 2, respectively, with analogous expressions for $z_n^{(2)}$ and $z_d^{(2)}$. The results indicate strong dependence on w, especially for the axisymmetric mode.

Finally, Fig. 4(d) presents plots of single-mode strengths as functions of $c^{(1)}$ for $z^{(2)} = 0.25$ and $w = 5$. We observe that the upper (+) estimates exhibit the expected trends, with the effective yield ranging from the strength of the stronger phase ($\tau_y^{(2)}$) for $c^{(1)} = 0$ to that of the weaker phase ($\tau_y^{(1)}$) for $c^{(1)} = 1$. On the other hand, the corresponding lower (−) estimates do tend to $\tau_y^{(1)}$ as $c^{(1)} \to 1$, but they do not approach $\tau_y^{(2)}$ as $c^{(1)} \to 0$. To understand this unexpected result [see also Suquet (1993)], it is important to note that, for $c^{(1)} = 0$, we are in a range of $z^{(2)}$ and w for which the inclusions (of material 1) look effectively rigid to the matrix (material 2). Otherwise, the effective yield strength would exhibit the expected behavior in the limit as $c^{(1)} \to 0$. Physically, the unusual result may be understood in the following terms. For sufficiently large contrast, even a small proportion of the weaker continuous matrix will lead to significant softening of the effective behavior (e.g. rigid inclusions in a fluid).

5. CONCLUDING REMARKS

This first part of this work has dealt with the development of effective potentials for the class of nonlinearly viscous composites with particulate ellipsoidal microstructures

(corresponding to two-phase materials with distributions of aligned ellipsoidal inclusions of one phase distributed in a matrix of another). These potentials are valid for general loading conditions and for arbitrary values of the volume fractions of the phases, aspect ratios of the inclusions and yield strength ratios. They will be used in Part II of this work as "instantaneous" potentials for the nonlinearly viscous composites with evolving microstructures, where the "current" values of the volume fractions of the phases and aspect ratios of the inclusions, characterizing the state of the microstructure, will be determined by the appropriate evolution law derived from standard kinematical relations.

The main results of this part of the work are the establishment of simple formulae for the effective potentials and yield functions, respectively, of two-phase nonlinearly viscous and rigid–perfectly plastic composites with particulate ellipsoidal microstructures. These general formulae are given in terms of one-dimensional optimization problems involving the explicit Hashin–Shtrikman estimates of Willis (1977, 1978) for the effective viscosity coefficient of linearly viscous composites with the same type of microstructures as the nonlinear composites. Computations were carried out for the special case of rigid–perfectly plastic composites with aligned spheroidal inclusions. In this case, the overall symmetry of the composite is transversely isotropic and the effective behavior may be expressed in terms of three independent modes: axisymmetric tension, transverse shear and longitudinal shear. The resulting yield surfaces are found to be weakly anisotropic and not too different from the classical upper bound estimates of Bishop and Hill, if the stronger phase is chosen to occupy the matrix phase. On the other hand, if the weaker phase is chosen to occupy the matrix phase, the resulting yield surfaces may be strongly anisotropic. For the particular cases of laminated and fiber-reinforced microstructures, the yield surfaces are found to be bi-modal in shape, with weak modes controlled by the weak phase (the longitudinal shear mode for the laminates and the transverse and longitudinal shear modes for the fiber composites) and strong modes controlled by the stronger phase (the axisymmetric and transverse shear modes for the laminates and the axisymmetric mode for the fiber composites). In addition, the yield surfaces of these materials with continuous reinforcement exhibit flat sectors and "corners". On the other hand, the yield surfaces of the composites with particulate reinforcement are relatively smooth. The main observation relating to the latter class of materials is that the optimal particle shape in terms of strengthening or weakening the composite depends strongly on the loading mode. We also note that results for more general ellipsoidal inclusion shapes have been given in Zaidman (1994).

We conclude by remarking that, at least judging by the comparisons made here with the numerical simulations of Moulinec and Suquet (1994a, b) for the special case of fiber-reinforced perfectly plastic composites, the model seems to be capable of predicting with reasonable accuracy the effective behavior of nonlinear composites. In particular, the model was able to capture the significantly nonlinear bi-modal character of the yield surfaces of fiber-reinforced composites. Another encouraging comparison was carried out recently by Gilormini (1995) in the context of statistically isotropic power-law composites. This author compared the predictions of Ponte Castañeda (1991) [see also Ponte Castañeda (1992) and Suquet (1993)] for this class of composites with the corresponding predictions of the classical self-consistent model of Hill (1965), as extended to nonlinearly viscous behavior by Hutchinson (1976), and found that for sufficiently large nonlinearity and contrast between the phases, the self-consistent estimates actually violate the Hashin–Shtrikman upper bounds of Ponte Castañeda (1991). Although the differences in the predictions of the two models are small in absolute terms, the mere fact that the new estimates are able to improve on those based on a well-established procedure make it plausible that the estimates given here for more general types of microstructures may actually be quite strong.

Acknowledgements—This work was supported by NSF grant MSS-92-02513 and by the NSF/MRL Program at the University of Pennsylvania under grant no. DMR91-20668. This manuscript was completed while one of the authors (P. P. C.) was a Visiting Professor at the Laboratoire de Mecanique des Solides, Ecole Polytechnique, Paris. Thanks are due to Mahesh Kailasam for useful comments on an earlier version of this manuscript.

REFERENCES

Bao, G., Hutchinson, J. W. and McMeeking, R. M. (1991). The flow stress of dual phase, non-hardening solids. *Mech. Mater.* **12,** 85–94.

Bishop, J. F. W. and Hill, R. (1951). A theory of the plastic distorsion of a polycrystalline aggregate under combined stresses. *Phil. Mag.* **42,** 414–427.

deBotton, G. and Ponte Castañeda, P. (1993). Elastoplastic constitutive relations for fiber-reinforced solids. *Int. J. Solids Structures* **30,** 1865–1890.

Drucker, D. C. (1959). On minimum weight design and strength of non-homogeneous plastic bodies. In *Non-homogeneity in Elasticity and Plasticity* (Edited by W. Olszak), pp. 139–146. Pergamon Press, New York.

Dvorak, G. J. and Bahei-El-Din, Y. A. (1987). A bimodal plasticity theory of fibrous composite materials. *Acta Mech.* **69,** 219–241.

Dvorak, G. J. and Bahei-El-Din, Y. A., Macheret, Y. and Liu, C. H. (1988). An experimental study of the elastic–plastic behavior of a fibrous composite. *J. Mech. Phys. Solids* **26,** 655–687.

Eshelby, J. D. (1957). The determination of the elastic field of an ellipsoidal inclusion, and related problems. *Proc. R. Soc. Lond. A* **241,** 376–396.

Gilormini, P. (1995). A shortcoming of the classical nonlinear extension of the self-consistent model. *C. R. Acad. Sci. Paris II* **320,** 115–122.

Hashin, Z. (1980). Failure criteria for unidirectional fiber composites. *ASME J. Appl. Mech.* **47,** 329–334.

Hashin, Z. and Shtrikman, S. (1963). A variational approach to the theory of the elastic behavior of multiphase materials. *J. Mech. Phys. Solids* **11,** 127–140.

Hill, R. (1963). Elastic properties of reinforced solids: some theoretical principles. *J. Mech. Phys. Solids* **11,** 357–352.

Hill, R. (1965) Continuum micromechanics of elastoplastic polycrystals. *J. Mech. Phys. Solids* **13,** 89–101.

Hill, R. (1967). The essential structure of constitutive laws for metal composites and polycrystals. *J. Mech. Phys. Solids* **15,** 79–95.

Hutchinson, J. W. (1976). Bounds and self-consistent estimates for creep of polycrystalline materials. *Proc. R. Soc. Lond. A* **348,** 101–127.

Li, G. and Ponte Castañeda, P. (1994). Variational estimates for the elastoplastic response of particle-reinforced metal–matrix composites. *Appl. Mech. Rev.* **47,** S77–94.

Milton, G. W. and Kohn, R. V. (1988). Variational bounds on the effective moduli of anisotropic composites. *J. Mech. Phys. Solids* **36,** 597–629.

Mori, T. and Tanaka, K. (1973). Average stress in matrix and average elastic energy of materials with misfitting inclusions. *Acta Metall.* **21,** 571–574.

Moulinec, H. and Suquet, P. (1994a). A fast numerical method for computing the linear and nonlinear mechanical properties of composites. *C. R. Acad. Sci. Paris II* **318,** 1417–1423.

Moulinec, H. and Suquet, P. (1994b). A FTT-based numerical method for computing the mechanical properties of composites from images of their microstructures. To appear in *Proc. IUTAM Symp. on Microstructure-Property Interactions in Composite Materials*, Alborg, Denmark.

Olson, T. (1994). Improvements on Taylor's upper bound for rigid–plastic composites. *Mater. Sci. Engng A* **175,** 15–19.

Ponte Castañeda, P. (1991). The effective mechanical properties of nonlinear isotropic solids. *J. Mech. Phys. Solids* **39,** 45–71.

Ponte Castañeda, P. (1992). New variational principles in plasticity and their application to composite materials. *J. Mech. Phys. Solids* **40,** 1757–1788.

Ponte Castañeda, P. and deBotton, G. (1992). On the homogenized yield strength of two-phase composites. *Proc. R. Soc. Lond. A* **438,** 419–431.

Ponte Castañeda, P. and Willis, J. R. (1988). On the overall properties of nonlinearly viscous composites. *Proc. R. Soc. Lond. A* **416,** 217–244.

Ponte Castañeda, P. and Zaidman, M. (1994). Constitutive models for porous materials with evolving microstructure. *J. Mech. Phys. Solids* **42,** 1459–1497.

Suquet, P. (1983). Analyse limite et homogénéisation. *C. R. Acad. Sci. Paris II* **295,** 1355–1358.

Suquet, P. (1993). Overall potentials and extremal yield surfaces of power law or ideally plastic composites. *J. Mech. Phys. Solids* **41,** 981–1002.

Talbot, D. R. S. and Willis, J. R. (1985). Variational principles for nonlinear inhomogeneous media. *IMA J. Appl. Math.* **35,** 39–54.

Talbot, D. R. S. and Willis, J. R. (1992). Some explicit bounds for the overall behavior of nonlinear composites. *Int. J. Solids Structures* **29,** 1981–1987.

Willis, J. R. (1977). Bounds and self-consistent estimates for the overall moduli of anisotropic composites. *J. Mech. Phys. Solids* **25,** 185–202.

Willis, J. R. (1978). Variational principles and bounds for the overall properties of composites. In *Continuum Models for Discrete Systems* (Edited by J. W. Provan), pp. 185–215. University of Waterloo Press.

Zaidman, M. (1994). Constitutive models for composite materials with evolving microstructures. Ph.D. Thesis, Department of Mechanical Engineering and Applied Mechanics, University of Pennsylvania.

Zaidman, M. and Ponte Castañeda, P. (1996). The finite deformation of nonlinear composite materials—II. Evolution of the microstructure. *Int. J. Solids Structures* **33,** 1287–1303.

APPENDIX: SPECIAL RESULTS FOR SPHEROIDAL INCLUSIONS

The expression for $\tilde{\mu}_0$ appearing in expression (23) for the case of aligned spheroidal inclusions of phase 1, with aspect ratios $w_1 = w_2 = w$, is given by:

$$\frac{\mu^{(2)}}{\tilde{\mu}_p} = \frac{e_1^{(2)} y^{(1)} + e_2^{(2)}}{e_3^{(2)} y^{(1)} + e_4^{(2)}}, \tag{A1}$$

where

$$\begin{aligned} e_1^{(2)} &= c^{(2)}(3h - 2w^2) - 4(1 - w^2) \\ e_2^{(2)} &= -c^{(2)}(3h - 2w^2) \\ e_3^{(2)} &= c^{(2)}(-4 + 3h + 2w^2) \\ e_4^{(2)} &= 2w^2 - 3c^{(2)}h + 2c^{(1)}(w^2 - 2). \end{aligned} \tag{A2}$$

The corresponding results for $\tilde{\mu}_n$ and $\tilde{\mu}_d$ are given by formulae completely analogous to eqn (A1), except that the $e_i^{(2)}$ $(i = 1, 2, 3, 4)$ must be replaced by the $f_i^{(2)}$ and $g_i^{(2)}$ below

$$\begin{aligned} f_1^{(2)} &= c^{(2)}(-2 + 3h - 2w^2 + 3hw^2) + 2(1 - w^2) \\ f_2^{(2)} &= c^{(2)}(2 - 3h + 2w^2 - 3hw^2) \\ f_3^{(2)} &= c^{(2)}(3h - 4w^2 + 3hw^2) \\ f_4^{(2)} &= c^{(2)}(2 - 3h)(1 + w^2) + 2c^{(1)}(1 - w^2), \end{aligned} \tag{A3}$$

$$\begin{aligned} g_1^{(2)} &= 2(1 - w^2) - 3c^{(2)}(h - 2w^2 + 2hw^2) \\ g_2^{(2)} &= 3c^{(2)}(h - 2w^2 + 2hw^2) \\ g_3^{(2)} &= c^{(2)}(2 - 3h + 4w^2 - 6hw^2) \\ g_4^{(2)} &= 3c^{(2)}(h - 2w^2 + 2hw^2) + 2c^{(1)}(1 - w^2). \end{aligned} \tag{A4}$$

In these last relations,

$$h(w) = \begin{cases} \dfrac{w[\cos^{-1}(w) - w(1 - w^2)^{1/2}]}{(1 - w^2)^{3/2}}, & \text{if} \quad w \leqslant 1, \\ \dfrac{w[-\cosh^{-1}(w) + w(w^2 - 1)^{1/2}]}{(w^2 - 1)^{3/2}}, & \text{if} \quad w \geqslant 1. \end{cases} \tag{A5}$$

We next record the corresponding results for the single-mode stresses, for the special cases of laminates, statistically isotropic and transversely isotropic fiber-reinforced composites [see Ponte Castañeda and deBotton (1992)]:

Laminates ($w = 0$)

$$\begin{aligned} &\tilde{\tau}_p = \tilde{\tau}_d = c^{(1)}\tau_y^{(1)} + c^{(2)}\tau_y^{(2)}, \text{ if } z^{(2)} < \infty, \\ &\tilde{\tau}_n = \tau_y^{(1)}, \text{ if } z^{(2)} < 1, \text{ or } \tilde{\tau}_n = \tau_y^{(2)}, \text{ if } z^{(2)} \geqslant 1. \end{aligned} \tag{A6}$$

Isotropic composites ($w = 1$)

$$\tilde{\tau}_p = \tilde{\tau}_n = \tilde{\tau}_d = \begin{cases} \dfrac{5c^{(1)}}{3 + 2c^{(1)}}\tau_y^{(1)} + \dfrac{3c^{(2)}}{3 + 2c^{(1)}}\sqrt{\left(1 + \dfrac{2c^{(1)}}{3}\right)(\tau_y^{(2)})^2 - \dfrac{2c^{(1)}}{3}(\tau_y^{(1)})^2} & \text{if } z^{(2)} < \dfrac{5}{2}\sqrt{\dfrac{2}{2 + 3c^{(1)}}}, \\ \sqrt{1 + \frac{3}{2}c^{(1)}}\,\tau_y^{(2)} & \text{if } z^{(2)} \geqslant \dfrac{5}{2}\sqrt{\dfrac{2}{2 + 3c^{(1)}}}. \end{cases} \tag{A7}$$

Fiber composites ($w = \infty$)

$$\tilde{\tau}_d = c^{(1)}\tau_y^{(1)} + c^{(2)}\tau_y^{(2)}, \text{ if } z^{(2)} < \infty,$$

$$\tilde{\tau}_p = \tilde{\tau}_n = \begin{cases} \dfrac{2c^{(1)}}{1 + c^{(1)}}\tau_y^{(1)} + \dfrac{c^{(2)}}{1 + c^{(1)}}\sqrt{(1 + c^{(1)})(\tau_y^{(2)})^2 - c^{(1)}(\tau_y^{(1)})^2} & \text{if } z^{(2)} < 2\sqrt{\dfrac{1}{1 + c^{(1)}}}, \\ \sqrt{1 + c^{(1)}}\,\tau_y^{(2)} & \text{if } z^{(2)} \geqslant 2\sqrt{\dfrac{1}{1 + c^{(1)}}}. \end{cases} \tag{A8}$$

We note that the above results have assumed that the inclusion and matrix phases are made up of materials 1 and 2, respectively. If the roles of the matrix and inclusion are reverted, the above expressions apply with superscripts (1) and (2) interchanged.